

# The Landé $g$ factors for the $6S_{1/2}$ , $5D_{3/2,5/2}$ states of $Ba^+$ ions

Bing-Bing Li<sup>1</sup>, Jun Jiang<sup>1,\*</sup>, Lei Wu<sup>1</sup>, Deng-Hong Zhang<sup>1,2</sup>, and Chen-Zhong Dong<sup>1</sup>

<sup>1</sup>Key Laboratory of Atomic and Molecular Physics and Functional Materials of Gansu Province, College of Physics and Electronic Engineering, Northwest Normal University, Lanzhou 730070, P. R. China and

<sup>2</sup>College of Electronic Information and Electronic Engineering, Tianshui Normal University, Lanzhou 741000, P. R. China

The Landé  $g$  factors of  $Ba^+$  are very important in high-precision measurement physics. The wave functions, energy levels, and Landé  $g$  factors for the  $6s$   $^2S_{1/2}$  and  $5d$   $^2D_{3/2,5/2}$  states of  $Ba^+$  ions were calculated using the multi-configuration Dirac-Hartree-Fock (MCDHF) method and the Model-QED method. The contributions of the electron correlation effects and quantum electrodynamics (QED) effects were discussed in detail. The transition energies are in excellent agreement with the experimental results, with differences of approximately  $5 \text{ cm}^{-1}$ . The presently calculated  $g$  factor of 2.0024905(16) for the  $6S_{1/2}$  agrees very well with the available experimental and theoretical results, with a difference at a level of  $10^{-6}$ . For the  $5D_{3/2,5/2}$  states, the present results of 0.7993961(126) and 1.2003942(190) agree with the experimental results of 0.7993278(3) [Phys. Rev. A 54, 1199(1996)] and 1.20036739(14) [Phys. Rev. Lett. 124, 193001 (2020)] very well, with differences at the level of  $10^{-5}$ .

## I. INTRODUCTION

The Landé  $g$  factors are very important in high-precision measurement physics, including applications in atomic clock [1, 2], quantum computation [3, 4], and quantum information [5–7]. They also play a significant role in exploring high-order QED [8] and electron correlation effects [9, 10], as well as in testing the accuracy of theoretical methods. For few-electron systems, such as H-like [11–13], Li-like [14–16] systems, both theoretical and experimental results have achieved remarkable agreement [11, 17–20]. The two-loop QED effects [13, 15, 21, 22], screened QED effects [23], higher-order electron correlation effects [18, 24], and higher-order nuclear recoil effects [25–27] have been identified as crucial. However, for many-electron systems, high-precision theoretical calculations remain challenging due to the complexity of electron correlations.

$Ba^+$  is a promising candidate for quantum computing, quantum information, and atomic clock research [28, 29]. Its ground state is  $6s$ , and the metastable excited  $5d$  states have lifetimes of 48 and 32 s for the  $5D_{3/2}$  and  $5D_{5/2}$  states, respectively [30, 31]. The  $6S_{1/2} - 5D_{5/2}$  transition is a clock transition with a high quality factor of  $5.4 \times 10^{15}$ . The  $g$  factor of the ground state  $6s_{1/2}$  has been measured with an uncertainty at the level of  $10^{-7}$  [32–34]. Recently, Arnold *et al.* [29] and Hoffman *et al.* [35] have measured the  $g$  factor of the  $5D_{5/2}$  state in Paul traps, achieving uncertainties at the levels of  $10^{-7}$  and  $10^{-6}$ , respectively.

Theoretically, Lindroth *et al.* have calculated the  $g$  factor of the ground state  $6S_{1/2}$  of  $Ba^+$  [32], and their theoretical results are in agreement with the most accurate experimental results at the level of  $10^{-6}$ . However, for the excited state of  $5D_{3/2}$ , there is only one theoretical

result available from Ref. [36], which agrees with the most accurate experimental results at a level of  $10^{-4}$ . To our knowledge, there are no theoretical results for the  $5D_{5/2}$  state available for comparison with recent experimental data. Therefore, highly accurate theoretical calculations of the  $g$  factors for these excited states are required.

In this work, the wave functions, energy levels, and  $g$  factors of the  $6S_{1/2}$  and  $5D_{3/2,5/2}$  states of  $Ba^+$  were calculated using the multi-configuration Dirac-Hartree-Fock (MCDHF) method and the Model-QED method. The electron correlation effects, Breit interactions, and QED effects were discussed in detail.

## II. THEORETICAL METHODS

The MCDHF method is described in detail in Refs. [37–39], here, we only provide a brief overview. In this method, the atomic state wave function (ASF) for a given parity  $P$ , total angular momentum  $J$  and its projection on the Z-axis  $M$  is expressed as a linear combination of symmetry-adapted configuration state wave functions (CSFs) [38], i.e.,

$$\Psi(\gamma P J M_J) = \sum_{j=1}^{N_{CSFs}} c_j \Phi(\gamma_j P J M_J), \quad (1)$$

where  $c_j$  is the mixing coefficient and  $\gamma$  represents other quantum numbers of the corresponding states. The single electron orbitals are optimized through the relativistic self-consistent method. Subsequently, the mixing coefficients are obtained by performing relativistic configuration interaction (RCI) calculations, i.e., by diagonalising the Hamiltonian matrix of the configuration state space. In this step, the Breit interaction, QED effects, and nuclear recoil corrections can be added in the Hamiltonian matrix.

\* phyjiang@yeah.net

The Breit interaction is written as [37, 38, 40],

$$H_{\text{Breit}} = - \sum_{i < j}^N [\boldsymbol{\alpha}_i \cdot \boldsymbol{\alpha}_j \frac{\cos(\omega_{ij} r_{ij}/c)}{r_{ij}} + (\boldsymbol{\alpha}_i \cdot \nabla_i)(\boldsymbol{\alpha}_j \cdot \nabla_j) \frac{\cos(\omega_{ij} r_{ij}/c) - 1}{\omega_{ij}^2 r_{ij}^2/c^2}], \quad (2)$$

where  $\boldsymbol{\alpha}_i$  is the Dirac matrix consisting of three  $4 \times 4$  matrices,  $\nabla$  is the momentum operator,  $c$  is the speed of light, and  $r_{ij}$  is the distance between electron  $i$  and electron  $j$ . The frequency  $\omega_{ij}$  corresponds to the virtual photon exchanged between the electrons. The value of  $\omega_{ij}$  can be the difference of single electron energies. If  $\omega_{ij} \rightarrow 0$ , the operator reduces to the frequency-independent Breit interaction.

The contribution of QED were calculated using the Model-QED method [41–43]. This method has been successfully applied to studies of various atomic systems [44–54]. The QED effect is represented by the sum of the self-energy and the vacuum polarization [41–43]. The vacuum polarization was calculated by the sum of the Uehling potential [55] and the Wichmann-Kroll potential [56]. The self-energy operator is written as [41, 43]

$$h^{\text{SE}} = h_{\text{loc}}^{\text{SE}} + h_{\text{nloc}}^{\text{SE}}. \quad (3)$$

Here,  $h_{\text{loc}}^{\text{SE}}$  is the quasi-local operator, while  $h_{\text{nloc}}^{\text{SE}}$  denotes the nonlocal operator, these two operators are depicted in detail in Refs. [41, 43].

The  $g$  factor can be written as [57]

$$g = \frac{1}{2\mu_B} \frac{\langle \Psi(\gamma P J) \parallel \mathbf{N}^{(1)} \parallel \Psi(\gamma P J) \rangle}{\sqrt{J(J+1)(2J+1)}}, \quad (4)$$

where the operator

$$\mathbf{N}^{(1)} = -i \sum_j \sum_{q=0,\pm 1} \sqrt{\frac{8\pi}{3}} r_j \boldsymbol{\alpha}_j \cdot \mathbf{Y}_{1q}^{(0)}(\hat{\mathbf{r}}_j). \quad (5)$$

Here,  $\mathbf{Y}_{1q}^{(0)}$  is the vector spherical harmonic [58]. The QED correction due to the anomalous magnetic moment of the electron can be written as [57, 58],

$$\Delta g_{\text{QED}} = \frac{(g_s - 2) \langle \Psi(\gamma P J) \parallel \sum_j \Delta \mathbf{N}_j^{(1)} \parallel \Psi(\gamma P J) \rangle}{2\sqrt{J(J+1)(2J+1)}}, \quad (6)$$

where  $g_s = 2.0023193$  [59]. The operator  $\Delta \mathbf{N}_j^{(1)} = \beta_j \boldsymbol{\Sigma}_j$  and  $\boldsymbol{\Sigma}_j$  is the relativistic spin matrix.

### III. RESULTS AND DISCUSSION

#### A. energy levels

In order to accurately deal with the effects of electron correlation, three different correlation models, designated as Model A, Model B, and Model C, were employed. In Model A, the calculations were performed

using the single-reference configurations  $5s^2 5p^6 6s$  and  $5s^2 5p^6 5d$ , with the  $5p$ ,  $5d$ , and  $6s$  electrons set as active electrons. The configuration space was subsequently generated through single and double (SD) excitations from the occupied orbitals of the reference configurations to unoccupied (virtual) orbitals. The virtual orbitals were constrained to principal quantum numbers  $n_{\text{max}} \leq 9$  and orbital quantum numbers  $l \leq 5$  (i.e., the angular symmetries are  $s, p, d, f, g$ ). In this model, the core-valence (CV) electron correlation effects between the  $5p$  core electrons and the  $6s$  or  $5d$  valence electrons were considered. Model B was based on Model A, and included the  $5s$  core electrons as active electrons. This model extended Model A by incorporating the CV electron correlations between the  $5s$  core electrons and the  $6s$  and  $6d$  valence electrons, as well as the core-core (CC) electron correlations between the  $5s$  and  $5p$  electrons. The third model, Model C, incorporated higher-order electron correlations through SD excitations from multi-reference (MR) configurations. The configurations that significantly contributed to the wave function were selected as reference configurations. These reference configurations included  $5s^2 5p^6 6s_1$ ,  $5s^2 5p^6 5d_1$ ,  $5s^2 5p^4 5d_1 6s_1 6d_1$ ,  $5s^2 5p^5 5d_1 6p_1$ ,  $5s^2 5p^4 5d^2 6s_1$  and  $4d^9 5s^2 5p^6 6d_1 6s_1$ . The subscript denotes the maximum number of electrons that can be excited. Table 1 lists the numbers of CSFs that expand with the principal quantum number  $n$ . It should be noted that in Model C, the configurations that do not interact with  $6S_{1/2}$  and  $5D_{3/2,5/2}$  were eliminated by using the program "rcsfinteract" in the GRASP2018 [60]. In this model, the  $4d$  orbital was open, allowing the calculation to include the CC and CV correlations of the  $4d$  electrons.

Table 2 shows the convergence of the transition energies with the expansion of the configuration space. It can be seen that the transition energies calculated in each model converged very well when  $n_{\text{max}}$  was increased to 9. To illustrate the convergence of the different correlation models, Fig. 1 shows the difference of the transition energies between the calculated results for each correlation model with  $n_{\text{max}} = 9$  and the NIST standard values that are 4874, 5675, and 801  $\text{cm}^{-1}$  for the  $5D_{3/2} - 6S_{1/2}$ ,  $5D_{5/2} - 6S_{1/2}$ , and  $5D_{5/2} - 5D_{3/2}$  transitions, respectively. It is evident that Model C provides very good results. The difference between Dirac-Fock (DF) and Model A indicates the CV and CP correlations for the  $5p$  orbitals, which accounted for  $-10\%$  of the transition energy. The contribution of CV and CC correlations involving the  $5p$  orbital is about  $-6\%$ , which was obtain by the difference between Model A and Model B. Similarly, the contribution of CV and CC correlations involving the  $4d$  orbital, along with partial triple- and quadruple-excitations, is  $-2\%$  which was derived from the difference between Model B and Model C.

Then, we further calculated the Breit interactions, QED effects, and nuclear recoil by re-diagonalizing the Hamiltonian matrix on the basis of Model C with  $n_{\text{max}}=9$ . The matrix elements of self-energy and vacuum polarization were calculated using Model-QED

TABLE I. The number of CSF for the  $6S_{1/2}$ ,  $5D_{3/2,5/2}$  states of  $Ba^+$  ions in Model A, B, and C.

$n_{max}$	$6S_{1/2}$	$5D_{3/2}$	$5D_{5/2}$
Model A			
6	3 409	6 160	7 820
7	7 976	14 397	18 219
8	14 525	26 188	33 058
9	23 056	41 533	52 337
Model B			
6	6 331	11 447	14 550
7	14 889	26 877	34 016
8	27 125	48 893	61 690
9	43 039	77 495	97 572
Model C			
6	194 770	370 667	482 445
7	442 030	876 772	1 170 127
8	780 002	1 591 337	2 153 107
9	1 208 686	2 514 362	3 431 385

TABLE II. The convergence of transition energies of the  $6S_{1/2}$ ,  $5D_{3/2,5/2}$  states of  $Ba^+$  ions calculated using Model A, B, and C, respectively. (in  $cm^{-1}$ )

$n_{max}$	$5D_{3/2} - 6S_{1/2}$	$5D_{5/2} - 6S_{1/2}$	$5D_{5/2} - 5D_{3/2}$
Model A			
6	4887	5659	771
7	5316	6081	766
8	5360	6124	764
9	5367	6131	763
Model B			
6	4528	5308	780
7	4970	5743	773
8	5036	5807	770
9	5048	5818	770
Model C			
6	4683	5497	813
7	4945	5758	813
8	4945	5762	817
9	4925	5742	818

program[41, 42]. These matrix elements were then added to the Hamiltonian matrix, and the QED contributions to the energy levels and wave functions were obtained through diagonalization. Table 3 presents the individual contributions of the Breit interaction, QED effects and total transition energies for the  $5D_{3/2} - 6S_{1/2}$  and  $5D_{5/2} - 6S_{1/2}$  states, along with a comparison to some available results. Two types of Breit interactions, namely frequency-independent ( $\omega \rightarrow 0$ ) and frequency-dependent Breit interactions, were calculated in the present work. For the frequency-dependent Breit interactions calculations, the frequencies were still set to zero for virtual orbitals. It can be seen that the contribution of the Breit interaction comes mainly from the frequency-independent term, while the correction for  $\omega \neq 0$  is negligible. Additionally, the contributions of nuclear recoil was also assessed and found to be negligible, with a magnitude of less than  $0.1 cm^{-1}$ . The final energy levels labeled "Total", which included the contributions

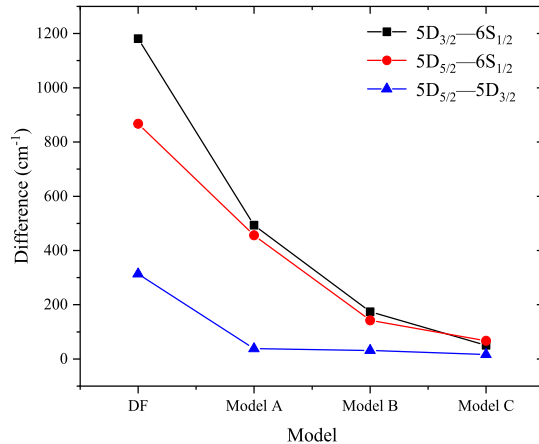


FIG. 1. Difference of the transition energies between the calculated results for each correlation model with  $n_{max} = 9$  and the NIST standard values that are 4874, 5675, and 801  $cm^{-1}$  for the  $5D_{3/2} - 6S_{1/2}$ ,  $5D_{5/2} - 6S_{1/2}$ , and  $5D_{5/2} - 5D_{3/2}$  transitions. DF is the results calculated using Dirac-Fock energies.

from the electronic correlation effects, Breit interactions, QED effects, show excellent agreement with the results of the NIST tabulation [61].

## B. Landé $g$ factor

Ignoring the electron correlation effects, QED effects and nuclear recoil, the  $g$  factor is reduced to the analytical Dirac value [64]

$$g_D = \frac{\kappa}{2J(J+1)}(2\kappa\varepsilon_{n\kappa} - 1), \quad (7)$$

where  $\varepsilon_{n\kappa}$  is the Dirac energy of the orbital and  $\kappa$  is the relativistic quantum number. For the states  $6S_{1/2}$ ,  $5D_{3/2}$ , and  $5D_{5/2}$  of the  $Ba^+$ , the  $g_D$  are 1.9968281, 0.7963948, and 1.1965435, respectively.

Table 4 shows the convergence of our calculated  $g$  factors using Eq. (4) as the maximum principal quantum number  $n_{max}$  increased in Model C. The contributions of electron correlation effects were obtained from the difference between the calculated  $g$  factor and the  $g_D$  values. When the configuration space reached  $n_{max} = 9$ , this contribution converges to a level of  $10^{-6}$ .

We also evaluated the contributions of the negative-energy states. The estimation method is similar to our previous calculations of the  $g$  factor for  $Ar^{13+}$  and Li-like  $Sn^{47+}$  and  $Bi^{80+}$  ions [65, 66]. The negative-energy orbitals were calculated by the relativistic configuration interaction plus core polarization (RCICP) method [67]. We then performed the RCI calculations again, substituting the positive energy orbitals for the negative-energy

TABLE 3. Transition energy (in  $\text{cm}^{-1}$ ) of the  $6D_{1/2}$ ,  $5D_{3/2,5/2}$  states of  $\text{Ba}^+$ . Breit( $\omega = 0$ ) and Breit( $\omega \neq 0$ ) represent the contributions from the frequency-independent and frequency-dependent interactions, respectively. The "Total" is the sum of CI, Breit( $\omega \neq 0$ ) and QED contributions. The "SD" represents the single-double (SD) all-order method. The "CP+CI" and "SDCC+CI" represents correlation-potential (CP) method and linearized singledouble-coupled-cluster (SDCC) method combine configuration-interaction (CI) techniques, respectively.

Contribution	$5D_{3/2} - 6S_{1/2}$	$5D_{5/2} - 6S_{1/2}$	$5D_{5/2} - 5D_{3/2}$
CI	4924.7	5742.3	817.6
Breit( $\omega=0$ )	-55.4	-80.8	-25.5
Breit( $\omega \neq 0$ )	-55.6	-81.6	-25.9
CI+Breit( $\omega \neq 0$ )	4869.0	5660.7	791.7
QED	9.4	9.3	- 0.1
Total	4878.4(245)	5670.0(248)	791.6(252)
SD [62]	4762	5521	759
SDCC+CI [63]	4869	5736	867
CP+CI [63]	4750	5611	861
Exp. [61]	4873.852	5674.807	800.955

TABLE 4. The convergence of positive-energy states to the  $g$  factor of the  $6S_{1/2}$ ,  $5D_{3/2}$ ,  $5D_{5/2}$  states for  $\text{Ba}^+$  ions calculated using Model C.  $\Delta g_{PS}$  represents the contribution of positive-energy states.  $g_D$  is the Dirac value.

$n_{max}$	$6S_{1/2}$		$5D_{3/2}$		$5D_{5/2}$	
	$g_D=1.9968281$		$g_D=0.7963948$		$g_D=1.1965435$	
	$g$	$\Delta g_{PS}=g-g_D$	$g$	$\Delta g_{PS}=g-g_D$	$g$	$\Delta g_{PS}=g-g_D$
6	2.0001674	0.0033393	0.7998653	0.0034705	1.1999431	0.0033996
7	2.0001617	0.0033336	0.7998623	0.0034674	1.1999382	0.0033948
8	2.0001680	0.0033399	0.7998610	0.0034662	1.1999364	0.0033930
9	2.0001678	0.0033397	0.7998604	0.0034656	1.1999355	0.0033921

orbitals. For the  $6S_{1/2}$ ,  $5D_{3/2}$ , and  $5D_{5/2}$  states, the contributions converged to 0.0000063,  $-0.0000009$ , and  $-0.0000047$ , respectively.

Table 5 lists the individual contributions to the  $g$  factors from different effects and compares them with existing theoretical and experimental results. The contributions of QED effects, denoted as " $\Delta g_{QED}$ ", were calculated using Eq. (6). For the  $6S_{1/2}$  ground state, the accuracy of the total  $g$  factors for all theoretical and experimental results reaches  $10^{-6}$ , demonstrating excellent consistency within their respective uncertainty ranges. Our calculated results show a difference of  $6 \times 10^{-7}$  from the theoretical result reported by Lindroth *et al.* [32]. Notably, our results are in excellent agreement with the experimental result from Ref. [34], with a difference of less than  $10^{-7}$ .

For the excited state  $5D_{3/2}$ , three experimental results [32, 36, 68] and one theoretical result [36] are available. The difference between the two most accurate experiments [36, 68] is  $1.6 \times 10^{-5}$ . The discrepancy between our result and the result of the most accurate experiment [36] is  $6.6 \times 10^{-5}$ , representing approximately an order of magnitude improvement in the accuracy of the result reported in Ref. [36]. For the  $5D_{5/2}$  state, three sets of experimental results are available for comparison. The difference between the two most accurate experiments [29, 35] is  $5 \times 10^{-6}$ . The difference between

our theoretical results and the most recent experimental results [29] is  $2.7 \times 10^{-5}$ . The primary sources of this discrepancy are the higher-order electron correlation effects and higher-order QED effects.

#### IV. CONCLUSIONS

The wave function, energy levels, and  $g$  factors for the  $6S_{1/2}$ , and  $5D_{3/2,5/2}$  states of  $\text{Ba}^+$  ions were calculated using the MCDHF method and Model-QED method. The electron correlation effects were investigated in detail using three different correlation models. The contribution of CV and CC correlation effect of  $5p$ ,  $5s$ , and  $4d$  electrons (along with partial triple- and quadruple-excitations) to the transition energies, reach  $-10\%$ ,  $-6\%$ , and  $-2\%$ , respectively. By including Breit interactions and QED effects, the differences between the currently calculated transition energies and the NIST standard values are reduced to approximately  $5 \text{ cm}^{-1}$ . In the calculation of the Landé  $g$  factors, the contributions from both positive and negative energy states and QED effects were analyzed. The present results show in good agreement with the experimental results, with differences at the level of  $10^{-6}$  and  $10^{-5}$  for the  $6S_{1/2}$  and  $5D_{3/2,5/2}$  states, respectively.

The current calculations demonstrates significantly improved accuracy compared to existing theoretical calculations and showed good agreement with the most pre-

TABLE 5. The  $g$  factor of the states  $6S_{1/2}$ ,  $5D_{3/2}$ ,  $5D_{5/2}$  for  $Ba^+$  ions. The "Total" represent the sum of  $g_D$ ,  $\Delta g_{PS}$ ,  $\Delta g_{NS}$  and  $\Delta g_{QED}$ .  $\Delta g_{NS}$  represents the contribution of the negative-energy states. The results of  $\Delta g_{QED}$  are calculated using Eq. (6).

	$6S_{1/2}$	$5D_{3/2}$	$5D_{5/2}$
$g_D$	1.9968281	0.7963948	1.1965435
$\Delta g_{PS}$	0.0033397	0.0034656	0.0033921
$\Delta g_{NS}$	0.0000063	-0.0000009	-0.0000047
$\Delta g_{QED}$	0.0023205	-0.0004641	0.0004641
Total	2.0024905(16)	0.7993961(126)	1.2003942(190)
Exp.	2.0024922(10) [36]	0.800(9) [32]	1.20036739(24) [29]
	2.00249192(3) [33]	0.7993278(3) [36]	1.200372(4)stat(7)sys [35]
	2.0024906(12) [34]	0.799311(4) [68]	1.2020(5) [69]
Theory	2.0024911(30) [32]	0.79946 [36]	

cise experimental results. However, discrepancies persist between theoretical and experimental values for the excited states  $5D_{3/2}$  and  $5D_{5/2}$ , where the theoretical results lie outside the experimental error bars. The difference, on the order of  $10^{-5}$ , is two orders of magnitude larger than the experimental precision of  $10^{-7}$ . Therefore, further advanced theoretical works are still needed, particularly regarding the higher-order electron correlation effects, two-loop QED effects, and relativistic nuclear recoil effects. These effects have been proven critical in few-electron systems but remain challenging to address in

many-electron systems due to computational complexity.

## V. ACKNOWLEDGMENTS

This work has been supported by the National key Research and Development Program of China under Grant No.2022YFA1602500, the National Natural Science Foundation of China under Grant No.12174316, 1236040286, 12404306.

- 
- [1] J. Han, Y. Yu, B. Sahoo, J. Zhang, and L. Wang, Roles of electron correlation effects for the accurate determination of  $g$  factors of low-lying states of  $cd+113$  and their applications to atomic clocks, *Physical Review A* **100**, 042508 (2019).
- [2] Z. Ma, B. Zhang, Y. Huang, R. Hu, M. Zeng, K. Gao, and H. Guan, Precision determination of the oscillating-magnetic-field-induced second-order zeeman shift of a single- $^{40}Ca^+$ -ion optical clock, *Phys. Rev. A* **110**, 063102 (2024).
- [3] M. R. Dietrich, N. Kurz, T. Noel, G. Shu, and B. B. Blinov, Hyperfine and optical barium ion qubits, *Phys. Rev. A* **81**, 052328 (2010).
- [4] R. Hanson and D. D. Awschalom, Coherent manipulation of single spins in semiconductors, *Nature* **453**, 1043 (2008).
- [5] D. Hucul, J. E. Christensen, E. R. Hudson, and W. C. Campbell, Spectroscopy of a synthetic trapped ion qubit, *Phys. Rev. Lett.* **119**, 100501 (2017).
- [6] I. V. Inlek, C. Crocker, M. Lichtman, K. Sosnova, and C. Monroe, Multispecies trapped-ion node for quantum networking, *Phys. Rev. Lett.* **118**, 250502 (2017).
- [7] D. Leibfried, M. D. Barrett, T. Schaetz, J. Britton, J. Chiaverini, W. M. Itano, J. D. Jost, C. Langer, and D. J. Wineland, Toward Heisenberg-Limited Spectroscopy with Multiparticle Entangled States, *Science* **304**, 1476 (2004).
- [8] V. A. Yerokhin, K. Pachucki, M. Puchalski, Z. Harman, and C. H. Keitel, Electron-correlation effects in the  $g$  factor of light li-like ions, *Phys. Rev. A* **95**, 062511 (2017).
- [9] V. Yerokhin, K. Pachucki, M. Puchalski, Z. Harman, and C. Keitel, Electron-correlation effects in the  $g$  factor of light li-like ions, *Physical Review A* **95**, 062511 (2017).
- [10] D. Zinenko, D. Glazov, V. Kosheleva, A. Volotka, and S. Fritzsche, Electron correlation effects on the  $g$  factor of lithiumlike ions, *Physical Review A* **107**, 032815 (2023).
- [11] H. Häffner, T. Beier, N. Hermanspahn, H.-J. Kluge, W. Quint, S. Stahl, J. Verdú, and G. Werth, High-accuracy measurement of the magnetic moment anomaly of the electron bound in hydrogenlike carbon, *Physical review letters* **85**, 5308 (2000).
- [12] V. Hannen, J. Vollbrecht, Z. Anđelković, C. Brandau, A. Dax, W. Geithner, C. Geppert, C. Gorges, M. Hammen, S. Kaufmann, *et al.*, Lifetimes and  $g$ -factors of the hfs states in h-like and li-like bismuth, *Journal of Physics B: Atomic, Molecular and Optical Physics* **52**, 085003 (2019).
- [13] J. Morgner, B. Tu, C. M. König, T. Sailer, F. Heiße, H. Bekker, B. Sikora, C. Lyu, V. A. Yerokhin, Z. Harman, J. R. Crespo López-Urrutia, C. H. Keitel, S. Sturm, and K. Blaum, Stringent test of QED with hydrogen-like tin, *nature* **622**, 53 (2023), arXiv:2307.06613 [physics.atom-ph].
- [14] D. A. Glazov, F. Köhler-Langes, A. V. Volotka, K. Blaum, F. Heiße, G. Plunien, W. Quint, S. Rau, V. M. Shabaev, S. Sturm, and G. Werth,  $g$  factor of lithiumlike silicon: New challenge to bound-state qed, *Phys. Rev. Lett.* **123**, 173001 (2019).
- [15] D. Glazov, V. Shabaev, I. Tupitsyn, A. Volotka, V. Yerokhin, P. Indelicato, G. Plunien, and G. Soff,  $g$  factor of lithiumlike ions, *Nuclear Instruments and Meth-*

- ods in Physics Research Section B: Beam Interactions with Materials and Atoms **235**, 55 (2005), the Physics of Highly Charged Ions.
- [16] V. Kosheleva, A. Volotka, D. Glazov, D. Zinenko, and S. Fritzsche,  $g$  factor of lithiumlike silicon and calcium: resolving the disagreement between theory and experiment, Physical Review Letters **128**, 103001 (2022).
- [17] J. Verdú, S. Djekić, S. Stahl, T. Valenzuela, M. Vogel, G. Werth, T. Beier, H.-J. Kluge, and W. Quint, Electronic  $g$  factor of hydrogenlike oxygen  $o\ 7+16$ , Physical review letters **92**, 093002 (2004).
- [18] S. Sturm, A. Wagner, B. Schabinger, J. Zatorski, Z. Harman, W. Quint, G. Werth, C. H. Keitel, and K. Blaum,  $g$  factor of hydrogenlike silicon  $si\ 13+28$ , Physical review letters **107**, 023002 (2011).
- [19] S. Sturm, A. Wagner, M. Kretzschmar, W. Quint, G. Werth, and K. Blaum,  $g$ -factor measurement of hydrogenlike  $28\ si\ 13+$  as a challenge to qed calculations, Physical Review A—Atomic, Molecular, and Optical Physics **87**, 030501 (2013).
- [20] A. Wagner, S. Sturm, F. Köhler, D. A. Glazov, A. V. Volotka, G. Plunien, W. Quint, G. Werth, V. M. Shabaev, and K. Blaum,  $g$  factor of lithiumlike silicon  $si\ 11+28$ , Physical review letters **110**, 033003 (2013).
- [21] H. Cakir, V. A. Yerokhin, N. S. Oreshkina, B. Sikora, I. I. Tupitsyn, C. H. Keitel, and Z. Harman, QED corrections to the  $g$  factor of li- and b-like ions, Phys. Rev. A **101**, 062513 (2020).
- [22] U. D. Jentschura, Binding two-loop vacuum-polarization corrections to the bound-electron  $g$  factor, Physical Review A—Atomic, Molecular, and Optical Physics **79**, 044501 (2009).
- [23] D. A. Glazov, V. M. Shabaev, I. I. Tupitsyn, A. V. Volotka, V. A. Yerokhin, G. Plunien, and G. Soff, Relativistic and qed corrections to the  $g$  factor of li-like ions, Phys. Rev. A **70**, 062104 (2004).
- [24] I. A. Aleksandrov, D. A. Glazov, A. V. Malyshev, V. M. Shabaev, and I. I. Tupitsyn, Relativistic nuclear-recoil effect on the  $g$  factor of highly charged boronlike ions, Phys. Rev. A **98**, 062521 (2018).
- [25] T. Sailer, V. Debievre, Z. Harman, F. Heiße, C. König, J. Morgner, B. Tu, A. V. Volotka, C. H. Keitel, K. Blaum, *et al.*, Measurement of the bound-electron  $g$ -factor difference in coupled ions, Nature **606**, 479 (2022).
- [26] D. A. Glazov, A. V. Malyshev, V. M. Shabaev, and I. I. Tupitsyn, Interelectronic-interaction contribution to the nuclear recoil effect on the  $g$  factor of boronlike ions, Phys. Rev. A **101**, 012515 (2020).
- [27] A. Malyshev, I. Anisimova, D. Mironova, V. Shabaev, and G. Plunien, QED theory of the specific mass shift in few-electron atoms, Physical Review A **100**, 012510 (2019).
- [28] J. A. Sherman, W. Trimble, S. Metz, W. Nagourney, and N. Fortson, Progress on indium and barium single ion optical frequency standards, in *Digest of the LEOS Summer Topical Meetings, 2005*. (IEEE, 2005) pp. 99–100.
- [29] K. J. Arnold, R. Kaewuam, S. R. Chanu, T. R. Tan, Z. Zhang, and M. D. Barrett, Precision measurements of the  $^{138}\text{Ba}^+ 6s^2S_{1/2} - 5d^2D_{5/2}$  clock transition, Phys. Rev. Lett. **124**, 193001 (2020).
- [30] J. Gurell, E. Biémont, K. Blagoev, V. Fivet, P. Lundin, S. Mannervik, L.-O. Norlin, P. Quinet, D. Rostohar, P. Royen, and P. Schef, Laser-probing measurements and calculations of lifetimes of the  $5d\ ^2d_{5/2}$  and  $5d\ ^2d_{3/2}$  metastable levels in  $\text{Ba}^+$ , Phys. Rev. A **75**, 052506 (2007).
- [31] W. Nagourney, J. Sandberg, and H. Dehmelt, Shelved optical electron amplifier: Observation of quantum jumps, Phys. Rev. Lett. **56**, 2797 (1986).
- [32] E. Lindroth and A. Ynnerman, Ab initio calculations of  $g_j$  factors for Li,  $\text{Be}^+$ , and  $\text{Ba}^+$ , Phys. Rev. A **47**, 961 (1993).
- [33] G. Marx, G. Tommaseo, and G. Werth, Precise  $-$  and  $-$ factor measurements of  $\text{Ba}^+$  isotopes, The European Physical Journal D - Atomic, Molecular, Optical and Plasma Physics **4**, 279 (1998).
- [34] H. Knab, K. H. Knöll, F. Scheerer, and G. Werth, Experimental ground state  $g$ -factor of  $\text{Ba}^+$  in a penning ion trap, Zeitschrift für Physik D Atoms, Molecules and Clusters **25**, 205 (1993).
- [35] M. R. Hoffman, T. W. Noel, C. Aughter, A. Jayakumar, S. R. Williams, B. B. Blinov, and E. N. Fortson, Radio-frequency-spectroscopy measurement of the Landé  $g_J$  factor of the  $5D_{5/2}$  state of  $\text{Ba}^+$  with a single trapped ion, Phys. Rev. A **88**, 025401 (2013).
- [36] K. H. Knöll, G. Marx, K. Hübner, F. Schweikert, S. Stahl, C. Weber, and G. Werth, Experimental  $g_j$  factor in the metastable  $5d_{3/2}$  level of  $\text{Ba}^+$ , Phys. Rev. A **54**, 1199 (1996).
- [37] C. Froese Fischer, M. Godefroid, T. Brage, P. Jönsson, and G. Gaigalas, Advanced multiconfiguration methods for complex atoms: I. Energies and wave functions, J. Phys. B **49**, 182004 (2016).
- [38] P. Jönsson, G. Gaigalas, P. Rynkun, L. Radžiūtė, J. Ekman, S. Gustafsson, H. Hartman, K. Wang, M. Godefroid, C. Froese Fischer, *et al.*, Multiconfiguration dirac-tree-fock calculations with spectroscopic accuracy: Applications to astrophysics, Atoms **5**, 16 (2017).
- [39] I. Grant, Relativistic quantum theory of atoms and molecules, Springer series on atomic, Optical and Plasma Physics **40**, 173 (2007).
- [40] G. C. Rodrigues, M. A. Ourdane, J. Bieroń, P. Indelicato, and E. Lindroth, Relativistic and many-body effects on total binding energies of cesium ions, Phys. Rev. A **63**, 012510 (2000).
- [41] V. Shabaev, I. Tupitsyn, and V. Yerokhin, QEDmod: Fortran program for calculating the model Lamb-shift operator, Computer Physics Communications **189**, 175 (2015).
- [42] V. M. Shabaev, I. I. Tupitsyn, and V. A. Yerokhin, Model operator approach to the Lamb shift calculations in relativistic many-electron atoms, Phys. Rev. A **88**, 012513 (2013).
- [43] V. Shabaev, I. Tupitsyn, and V. Yerokhin, QEDmod: Fortran program for calculating the model Lamb-shift operator, Computer Physics Communications **223**, 69 (2018).
- [44] A. V. Malyshev, D. A. Glazov, V. M. Shabaev, I. I. Tupitsyn, V. A. Yerokhin, and V. A. Zaytsev, Model-qed operator for superheavy elements, Phys. Rev. A **106**, 012806 (2022).
- [45] I. S. Anisimova, A. V. Malyshev, D. A. Glazov, M. Y. Kaygorodov, Y. S. Kozhedub, G. Plunien, and V. M. Shabaev, Model-qed-operator approach to relativistic calculations of the nuclear recoil effect in many-electron atoms and ions, Phys. Rev. A **106**, 062823 (2022).
- [46] I. I. Tupitsyn, A. V. Malyshev, D. A. Glazov, M. Y. Kaygorodov, Y. S. Kozhedub, I. M. Savelyev, and V. M. Shabaev, Relativistic Calculations of the Chemical Properties of the Superheavy Element with  $Z = 119$  and Its Homologues, Optics and Spectroscopy **129**, 1038 (2021),

- arXiv:2103.15886 [physics.atom-ph].
- [47] V. M. Shabaev, I. I. Tupitsyn, M. Y. Kaygorodov, Y. S. Kozhedub, A. V. Malyshev, and D. V. Mironova, QED corrections to the  ${}^2p_{1/2} - {}^2p_{3/2}$  fine structure in fluorinelike ions: Model lamb-shift-operator approach, *Phys. Rev. A* **101**, 052502 (2020).
- [48] A. V. Volotka, M. Bilal, R. Beerwerth, X. Ma, T. Stöhler, and S. Fritzsche, QED radiative corrections to the  ${}^2p_{1/2} - {}^2p_{3/2}$  fine structure in fluorinelike ions, *Phys. Rev. A* **100**, 010502(R) (2019).
- [49] R. Si, X. L. Guo, T. Brage, C. Y. Chen, R. Hutton, and C. F. Fischer, Breit and QED effects on the  $3d\ ^{93/22}D \rightarrow {}^2D_{5/2}$  transition energy in Co-like ions, *Phys. Rev. A* **98**, 012504 (2018).
- [50] J. Machado, C. I. Szabo, J. P. Santos, P. Amaro, M. Guerra, A. Gumberidze, G. Bian, J. M. Isac, and P. Indelicato, High-precision measurements of  $n = 2 \rightarrow n = 1$  transition energies and level widths in he- and be-like argon ions, *Phys. Rev. A* **97**, 032517 (2018).
- [51] V. A. Yerokhin, A. Surzhykov, and A. Müller, Relativistic configuration-interaction calculations of the energy levels of the  $1s^22l$  and  $1s2l2l'$  states in lithiumlike ions: Carbon through chlorine, *Phys. Rev. A* **96**, 042505 (2017).
- [52] I. I. Tupitsyn, D. V. Mironova, A. V. Malyshev, and V. M. Shabaev, Model operator approach to the relativistic Lamb shift calculations in many-electron atoms and highly charged molecular ions, *Int. J. Mass Spectrom* **408**, 76 (2017).
- [53] I. I. Tupitsyn, M. G. Kozlov, M. S. Safronova, V. M. Shabaev, and V. A. Dzuba, Quantum electrodynamical shifts in multivalent heavy ions, *Phys. Rev. Lett.* **117**, 253001 (2016).
- [54] B.-B. Li, J. Jiang, L. Wu, R.-K. Zhang, X.-J. Li, and C.-Z. Dong, The excitation energies and hyperfine structures for  $2l$ ,  $3l$  states in lithiumlike ions, *Journal of Physics B: Atomic, Molecular and Optical Physics* **57**, 115003 (2024).
- [55] L. W. Fullerton and G. A. Rinker, Accurate and efficient methods for the evaluation of vacuum-polarization potentials of order  $z\alpha$  and  $z\alpha^2$ , *Phys. Rev. A* **13**, 1283 (1976).
- [56] A. G. Fainshtein, N. L. Manakov, and A. A. Nekipelov, Vacuum polarization by a coulomb field. analytical approximation of the polarization potential, *Journal of Physics B: Atomic, Molecular and Optical Physics* **24**, 559 (1991).
- [57] K. T. Cheng and W. J. Childs, Ab initio calculation of  $4f^N6s^2$  hyperfine structure in neutral rare-earth atoms, *Phys. Rev. A* **31**, 2775 (1985).
- [58] V. B. A.I. Akhiezer, *Quantum electrodynamics* (Interscience Publishers, 1965).
- [59] V. M. Shabaev, D. A. Glazov, M. B. Shabaeva, V. A. Yerokhin, G. Plunien, and G. Soff, g factor of high-z lithiumlike ions, *Phys. Rev. A* **65**, 062104 (2002).
- [60] C. Froese Fischer, G. Gaigalas, P. Jönsson, and J. Bieroń, GRASP2018-A Fortran 95 version of the General Relativistic Atomic Structure Package, *Computer Physics Communications* **237**, 184 (2019).
- [61] A. Kramida, Yu. Ralchenko, J. Reader, and NIST ASD Team, NIST Atomic Spectra Database (ver. 5.10), (Online). Available: <https://physics.nist.gov/asd> (2022).
- [62] U. Safronova, Relativistic many-body calculation of energies, lifetimes, hyperfine constants, multipole polarizabilities, and blackbody radiation shift in ba 137 ii, *Physical Review A—Atomic, Molecular, and Optical Physics* **81**, 052506 (2010).
- [63] V. Dzuba, Combination of the single-double-coupled-cluster and the configuration-interaction methods: Application to barium, lutetium, and their ions, *Physical Review A* **90**, 012517 (2014).
- [64] S. A. Zapryagaev, Zeeman effect of the fine structure levels of a hydrogenlike atom, *Opt. Spectrosc.* **47**, 9 (1979).
- [65] L. Wu, J. Jiang, Z.-W. Wu, Y.-J. Cheng, G. Gaigalas, and C.-Z. Dong, Energy levels, absorption oscillator strengths, transition probabilities, polarizabilities, and  $g$  factors of  $ar^{13+}$  ions, *Phys. Rev. A* **106**, 012810 (2022).
- [66] M. Liu, B.-B. Li, L. Wu, and J. Jiang, The Landé  $g$  factors of highly charged  $Sn^{47+}$  and  $Bi^{80+}$  ions, *Phys. Scripta* **99**, 055406 (2024).
- [67] J. Jiang, J. Mitroy, Y. Cheng, and M. W. J. Bromley, Relativistic semiempirical-core-potential calculations of  $sr^+$  using laguerre and slater spinors, *Phys. Rev. A* **94**, 062514 (2016).
- [68] G. Werth, Hyperfine structure and g-factor measurements in ion traps, *Physica Scripta Volume T* **59**, 206 (1995).
- [69] N. Kurz, M. R. Dietrich, G. Shu, T. Noel, and B. B. Blinov, Measurement of the landé  $g$  factor of the  $5D_{5/2}$  state of ba ii with a single trapped ion, *Phys. Rev. A* **82**, 030501 (2010).